ELSEVIER

Polymer 43 (2002) 3533–3540

polymer

www.elsevier.com/locate/polymer

Influence of subphase on the orientation of helical peptides at interface

Kazuya Kitagawa[a], Tomoyuki Morita[a], Junzo Umemura[b], Shunsaku Kimura[a,*]

[a]*Department of Material Chemistry, Graduate School of Engineering, Kyoto University, Yoshida Honmachi, Sakyo-ku, Kyoto 606-8501, Japan*

[b]*Institute for Chemical Research, Kyoto University, Gokanosho, Uji, Kyoto 611-0011, Japan*

Dedicated to Professor Imanishi on the occasion of his retirement

Received 13 December 2001; received in revised form 4 January 2002; accepted 7 January 2002

Abstract

Boc-(L-Leu-Aib)$_n$-OBzl ($n = 8$, 12, 16; OBzl represents benzyl ester) was spread on water or a mixture of water and methanol (1/1 v/v) and the orientation of the helical peptides on subphase was investigated by FTIR-reflection–absorption spectroscopy. When the peptides were spread at a liquid phase on subphase, the peptides took a vertical orientation, which was not attainable by compression of peptide monolayers initially spread at a gas phase on subphase. However, the peptide monolayers on water could not be transferred on gold with keeping the vertical orientation. On the other hand, when the peptides were spread on a mixture of water and methanol, the orientation of helical peptides was closer to vertical than that on water and the monolayers were transferred repeatedly on gold to form multilayers with a vertical orientation. The suppression of orientation change upon transfer of the peptide monolayer is considered to be due to reduction of electrostatic interaction between the peptide and the image dipole when the peptide is spread on a mixture of water and methanol. © 2002 Published by Elsevier Science Ltd.

Keywords: Helical peptide; Molecular assembly; Interface

1. Introduction

Helical peptides are rod-shaped and easily assembled into two-dimensional array on substrates and at air/water interface [1–3]. However, the control of helix orientation in the assemblies is not an easy task and in most cases helices lie horizontally at the interface [4,5]. There are only a few reports on the vertically oriented helical peptides, for example, on gold by using a self-assembling technique [6–10] and at liquid (water)–liquid (hexane) interface [11]. Molecular designing based on primary amphiphilicity, which theoretically promotes vertical orientation of amphiphilic molecules at interface according to hydrophobicity gradient formed at interface, [12] was not so effective to overcome the difficulty except in the case of connecting a large hydrophilic moiety to hydrophobic helical peptide [13].

Horizontal orientation of helical peptides at interface may be due to stabilization by an attractive force with interface, which becomes larger with closer contact of the molecule to the surface. That is, molecules with dipole moment deposited on gold or water experience an electrostatic attractive force as if there was an image dipole at the same distance on the other side of the interface, i.e. gold or water [14]. Since this interaction energy is proportional to $(\varepsilon_w - \varepsilon_m)/(\varepsilon_w + \varepsilon_m)$ (ε_w and ε_m represent the dielectric constants of water (or gold) and monolayer, respectively), this contribution should decrease with lowering ε_w. Therefore, using subphase having a lower dielectric constant may lead to formation of vertically oriented monolayer. On the basis of this idea, helical peptides were spread on a mixture of water and methanol (1/1 v/v) and the orientation of the helical peptides was investigated.

2. Experimental

2.1. Materials

Peptides, Boc-(L-Leu-Aib)$_n$-OBzl ($n = 8$, 12, 16; OBzl represents benzyl ester; Fig. 1), were synthesized by a conventional liquid phase method as previously reported [10]. Identification of Boc-(L-Leu-Aib)$_{12}$-OBzl and Boc-(L-Leu-Aib)$_{16}$-OBzl was made by ^{1}H NMR and mass spectroscopy as described later together with analytical thin layer chromatography data that were obtained by

* Corresponding author. Tel.: +81-75-753-4868; fax: +81-75-761-8846.
E-mail address: shun@scl.kyoto-u.ac.jp (S. Kimura).

0032-3861/02/$ - see front matter © 2002 Published by Elsevier Science Ltd.
PII: S0032-3861(02)00044-7

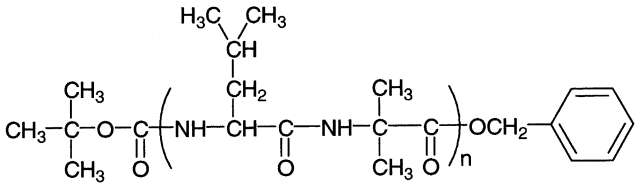

n=8; Boc-(L-Leu-Aib)$_8$-OBzl
n=12; Boc-(L-Leu-Aib)$_{12}$-OBzl
n=16; Boc-(L-Leu-Aib)$_{16}$-OBzl

Fig. 1. Molecular structure of Boc-(L-Leu-Aib)$_n$-OBzl ($n = 8$, 12, 16).

using Merck silica gel 60 F_{254} aluminum plates. The solvent systems used for TLC were (I) chloroform/methanol/acetic acid (95/5/3 v/v/v) and (II) chloroform/methanol (4/1 v/v).

2.1.1. Boc-(L-Leu-Aib)$_{12}$-OBzl

^{1}H NMR ($CDCl_3$, 400 MHz): δ (ppm) 0.80–0.98 (m, 72H, Leu CδH_3), 1.51 (s, 9H, Boc), 1.45–1.60 (m, 72H, Aib CH_3), 1.69 (m, 36H, Leu CβH_2 CγH), 3.88–4.23 (m, 12H, Leu CαH), 5.11 (dd, 2H, benzyl CH_2), 5.87 (s, 1H, urethane NH), 7.31 (AA′BB′, 5H, benzene), 7.5–7.9 (br, 23H, amide NH). FAB mass $[M + Na]^+ = 2610$ (calcd 2610). TLC: $R_f(I) = 0.32$, $R_f(II) = 0.85$.

2.1.2. Boc-(L-Leu-Aib)$_{16}$-OBzl

^{1}H NMR ($CDCl_3$, 400 MHz): δ (ppm) 0.80–0.98 (m, 96H, Leu CδH_3), 1.51 (s, 9H, Boc), 1.45–1.60 (m, 96H, Aib CH_3), 1.71 (m, 48H, Leu CβH_2 CγH), 3.83–4.24 (m, 16H, Leu CαH), 5.11 (dd, 2H, benzyl CH_2), 6.26 (s, 1H, urethane NH), 7.31 (AA′BB′, 5H, benzene), 7.5–8.1 (br, 31H, amide NH). FAB mass $[M + Na]^+ = 3403$ (calcd 3403). TLC: $R_f(I) = 0.32$, $R_f(II) = 0.77$.

2.2. Reflection–absorption spectroscopy measurements

The FTIR spectra were recorded on a Nicolet Magna 850 Fourier transform infrared spectrophotometer. For reflection–absorption spectroscopy (RAS) measurements of peptides on subphase and gold, a Specac 19650 monolayer/grazing angle accessory and a Harrick Model RMA-1DG/VRA reflection attachment were used, respectively. The *s*-polarized light used for RAS measurements on subphase was obtained through an ST Japan wire-grid polarizer. The incident angle was set at 65 and 80°, respectively, for measurements on subphase and gold. The number of interferogram accumulations was 300.

Gold substrates on clean slide glasses were prepared by thermal evaporation of chromium and gold with a 100 and a 1000 Å-thickness, respectively. All peripheral four sides of one surface of the substrates were masked by a Teflon tape to make a shallow trough on them. Water or a mixture of water and methanol (1/1 v/v) was put in and peptides in solution were spread on the subphase. The subphase was removed by slow evaporation at 40 °C in an oven to form a peptide layer on gold.

3. Results and discussion

3.1. π-A Isotherms of helical peptides at air–liquid interface

Boc-(L-Ala-Aib)$_8$-OMe and Boc-(L-Leu-Aib)$_8$-OBzl were previously reported to form two-dimensional crystals when they were spread on water subphase [4]. Especially, the monolayer of the latter peptide showed a well-packed molecular arrangement due to favorable interaction of isobutyl side chains of Leu residues. Thus, Boc-(L-Leu-Aib)$_n$-OBzl with three different molecular lengths were synthesized and studied here on monolayer formation at air–liquid interface.

The peptides were spread at a gas phase on water and π-*A* isotherms were monitored with compression of the monolayers (Fig. 2). The onset molecular areas of the surface-pressure increase as 3.2, 4.4 and 6.0 nm^2 with increasing the peptide length, which coincide with those corresponding to the cross-section along the helix axis 3.1, 4.7 and 6.2 nm^2 of the peptides [15]. All of the three helical peptides, therefore, formed a monolayer on water with laying down the helix axis parallel to water surface. This result is similar to those of other helical peptides [4], leading to a general interpretation that helical peptides strongly tend to lie down on water surface.

3.2. The relationship of tilt angles with ratios of amide I and amide II bands in RAS

s-Polarized light with incident angle of 65° was used for the RAS measurements of peptides on subphase. Principally, we followed the experimental procedures previously reported [16]. Under this condition, the tilt angles of helix axis from the surface normal are theoretically related with

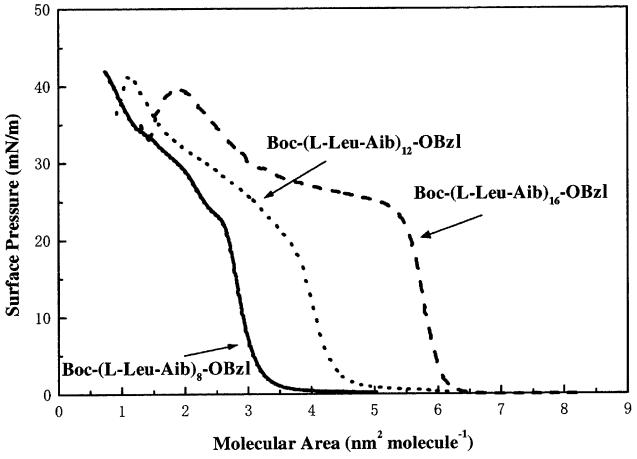

Fig. 2. π-A Isotherms of Boc-(L-Leu-Aib)$_n$-OBzl spread initially at a gas phase on water subphase.

the intensity ratios of amide I and II bands in the RAS spectra. The calculation was carried out by using the computer programs principally according to the mathematical formalism developed by Ohta and Ishida [17]. This formalism is based on the Abelès' matrix method [18] describing stratified layers of homogeneous films and involves appropriate modifications to interpret absorbing and anisotropic natures of layers [17,19].

An optical model of a three-phase (air/monolayer/water) system is considered. The optical property of the jth medium is described by the anisotropic complex refractive index,

$$\hat{n}_{jc} = n_{jc} + ik_{jc} \tag{1}$$

where $i^2 = -1$, n_j and k_j are the refractive index and the extinction coefficient of the jth medium, respectively, and c represents x, y, z coordinates. Although air ($j = 0$) is a non-absorbing and isotropic medium and water subphase ($j = 2$) is also isotropic, the peptide monolayer ($j = 1$) has uniaxial symmetry with the surface normal. The respective refractive indices are, thus, expressed as Eq. (2):

$$\hat{n}_{0x} = \hat{n}_{0y} = \hat{n}_{0z} = \hat{n}_0 = n_0 \qquad \hat{n}_{1x} = \hat{n}_{1y} \neq \hat{n}_{1z}$$
$$\hat{n}_{2x} = \hat{n}_{2y} = \hat{n}_{2z} = \hat{n}_2 \tag{2}$$

In the formalism, the relation among the amplitudes of the electric fields of incident wave E_0^+, reflected wave E_0^-, and transmitted wave after the monolayer E_2^+ is expressed as Eq. (3)

$$\begin{pmatrix} E_0^+ \\ E_0^- \end{pmatrix} = \frac{C_{0,1}\cdot C_{1,2}}{\hat{t}_{0,1}\cdot\hat{t}_{1,2}} \begin{pmatrix} E_2^+ \\ E_2^- \end{pmatrix} \tag{3}$$

with

$$C_{0,1} = \begin{bmatrix} \exp(-i\delta_0) & \hat{r}_{0,1}\exp(-i\delta_0) \\ \hat{r}_{0,1}\exp(i\delta_0) & \exp(i\delta_0) \end{bmatrix}$$
$$C_{1,2} = \begin{bmatrix} \exp(-i\hat{\delta}_1) & \hat{r}_{1,2}\exp(-i\hat{\delta}_1) \\ \hat{r}_{1,2}\exp(i\hat{\delta}_1) & \exp(i\hat{\delta}_1) \end{bmatrix} \tag{4}$$

where $\hat{r}_{j-1,j}$ and $\hat{t}_{j-1,j}$ are the Fresnel's reflection and transmission coefficients, respectively, between the $(j-1)$th and jth medium. These coefficients at the air/monolayer interface and the monolayer/water interface for s-polarized light are given by Eqs. (5) and (6):

$$\hat{r}_{0,1} = \frac{n_0\cos\theta_0 - \hat{n}_{1y}\cos\hat{\theta}_1}{n_0\cos\theta_0 + \hat{n}_{1y}\cos\hat{\theta}_1}$$
$$\hat{t}_{0,1} = \frac{2n_0\cos\theta_0}{n_0\cos\theta_0 + \hat{n}_{1y}\cos\hat{\theta}_1} \tag{5}$$

$$\hat{r}_{1,2} = \frac{n_{1y}\cos\hat{\theta}_1 - \hat{n}_2\cos\hat{\theta}_2}{n_{1y}\cos\hat{\theta}_1 + \hat{n}_2\cos\hat{\theta}_2}$$
$$\hat{t}_{1,2} = \frac{2\hat{n}_{1y}\cos\hat{\theta}_1}{\hat{n}_{1y}\cos\hat{\theta}_1 + \hat{n}_2\cos\hat{\theta}_2}. \tag{6}$$

The complex refractive angles $\hat{\theta}_j$ in the different medium are related to the incidence angle θ_0 by the Snell's law:

$$n_0\sin\theta_0 = \hat{n}_{1y}\sin\hat{\theta}_1 \qquad n_0\sin\theta_0 = \hat{n}_2\sin\hat{\theta}_2. \tag{7}$$

The terms δ_0 and $\hat{\delta}_1$ represent the phase thickness of air and the monolayer, respectively. δ_0 is equal to zero because air is the initial semi-infinite medium and $\hat{\delta}_1$ is expressed as Eq. (8)

$$\hat{\delta}_1 = 2\pi\nu d\hat{n}_{1y}\cos\hat{\theta}_1 \tag{8}$$

where ν and d represent the wavenumber of the incident light in the vacuum and the thickness of the monolayer, respectively. E_2^- is equal to zero in Eq. (3) because there is no reflection in the water subphase. By taking the matrix product as Eq. (9)

$$C_{01}\cdot C_{02} = \begin{bmatrix} a & b \\ c & d \end{bmatrix} \tag{9}$$

the reflection coefficient ($\hat{r}$) and reflectance (R) of the system are given by Eq. (10):

$$\hat{r} = \frac{E_0^-}{E_0^+} = \frac{c}{a} = \frac{\hat{r}_{0,1}\exp(-i\hat{\delta}_1) + \hat{r}_{1,2}\exp(i\hat{\delta}_1)}{\exp(-i\hat{\delta}_1) + \hat{r}_{0,1}\hat{r}_{1,2}\exp(i\hat{\delta}_1)}$$
$$R = |\hat{r}|^2. \tag{10}$$

On the other hand, the reflection coefficient ($\hat{r}_0$) and reflectance (R_0) in the absence of monolayer are easily obtained from the Fresnel's formula:

$$\hat{r}_0 = \frac{n_0\cos\theta_0 - \hat{n}_2\cos\hat{\theta}_2}{n_0\cos\theta_0 + \hat{n}_2\cos\hat{\theta}_2} \qquad R_0 = |\hat{r}_0|^2. \tag{11}$$

The absorbance of the system is, therefore, given as Eq. (12):

$$A = -\log_{10}\frac{R}{R_0}. \tag{12}$$

The simulation was performed with taking the refractive index of air being unity. The refractive index and extinction coefficient of water were taken from the literature values [20]. The anisotropic extinction coefficient of the peptide monolayer along y axis $k_y(\nu)$ was calculated by using a uniaxial symmetrical model, in which helical peptides are inclined from the surface normal direction (z) with a tilt angle (ϕ) and free rotation around z axis. The transition dipole moments of amide groups are expressed by two components, parallel (w) and perpendicular (u) to the helix axis [21]. The wavenumbers, maximum extinction coefficients and peak widths at half-height of the transition dipole moments of the amide I and II bands were taken from literature values which have been reported with those of poly-γ-benzyl-L-glutamate in a film [22,23]. The maximum values of k_{1y} of helical peptide with a tilt angle ϕ from surface normal are expressed by using the transition dipole

moments (I_w, I_u, II_w and II_u) as Eqs. (13) and (14):

$$k_{1y\ \max\ I_w} = \frac{1}{2}k_{\max\ I_w}\sin^2\phi$$
$$k_{1y\ \max\ I_u} = \frac{1}{4}k_{\max\ I_u}(1+\cos^2\phi) \tag{13}$$

$$k_{1y\ \max\ II_w} = \frac{1}{2}k_{\max\ II_w}\sin^2\phi$$
$$k_{1y\ \max\ II_u} = \frac{1}{4}k_{\max\ II_u}(1+\cos^2\phi). \tag{14}$$

Each extinction coefficient over the whole wavenumber is expressed as an antisymmetrical linear combination of two Lorentzian functions [24]

$$k_{1y\mathrm{TDM}}(\nu) = \frac{k_{1y\ \max\ \mathrm{TDM}}(\mathrm{fwhh}/2)^2}{(\nu-\nu_0)^2+(\mathrm{fwhh}/2)^2} - \frac{k_{1y\ \max\ \mathrm{TDM}}(\mathrm{fwhh}/2)^2}{(\nu+\nu_0)^2+(\mathrm{fwhh}/2)^2} \tag{15}$$

where fwhh is the peak width at half-height, ν_0 is the center wavenumber of the absorption band and TDM designates the component of the transition dipole moments (I_w, I_u, II_w, and II_u). The refractive indices are obtained from the Kramers–Kronig transformation of Eq. (15)

$$n_{1y\mathrm{TDM}}(\nu) = n_\infty - \frac{k_{1y\ \max\ \mathrm{TDM}}(\nu-\nu_0)(\mathrm{fwhh}/2)}{(\nu-\nu_0)^2+(\mathrm{fwhh}/2)^2} + \frac{k_{1y\ \max\ \mathrm{TDM}}(\nu+\nu_0)(\mathrm{fwhh}/2)}{(\nu+\nu_0)^2+(\mathrm{fwhh}/2)^2} \tag{16}$$

where n_∞ is the constant refractive index in the near-infrared region and was set to be 1.50 for the simulations. The sum of the extinction coefficients and refractive indices for the each transition dipole moment gives the complex refractive index of the peptide monolayer along y axis:

$$k_{1y}(\nu) = k_{1yI_w}(\nu) + k_{1yI_u}(\nu) + k_{1yII_w}(\nu) + k_{1yII_u}(\nu),$$
$$n_{1y}(\nu) = n_{1yI_w}(\nu) + n_{1yI_u}(\nu) + n_{1yII_w}(\nu) + n_{1yII_u}(\nu), \tag{17}$$
$$\hat{n}_{1y}(\nu) = n_{1y}(\nu) + Ik_{1y}(\nu).$$

The simulated RAS spectra of a helical peptide monolayer with varying the tilt angle of the helix axis from the surface normal are shown in Fig. 3. The relationship between the intensity ratios of the amide I and II bands and the tilt angles is shown in Fig. 4. The thickness of the peptide monolayer in the simulations is set to be 3.0 nm, which does not influence the ratio of the band intensities.

3.3. RAS measurements on subphase

RAS spectra of the helical peptides spread on water were measured with changing the preparation process of the peptide monolayers. The effects of solvent used for peptide stock solution, surface area for peptides to be spread, and monolayer compression on orientation of the helical axis were investigated.

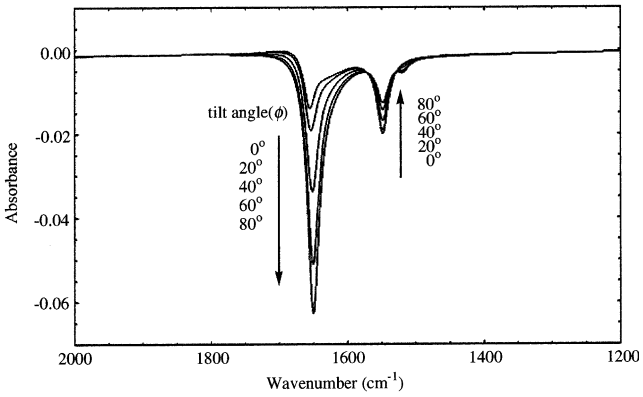

Fig. 3. The simulated RAS spectra in the region of amide I and II bands with changing the tilt angles of the helix axis from surface normal.

These peptides cannot take a vertical orientation on water subphase just by the conventional compression procedure of the peptide monolayer spread at a gas phase (Fig. 2). However, the situation became different when the peptides were spread at a limited area of water subphase (Fig. 5). The intensity ratio of amide I and II bands is less than the critical value of 4.0 corresponding to the random orientation. The intensity ratios of amide I and II bands and the tilt angles evaluated from the relationship shown in Fig. 4 are summarized in Table 1. Among the three peptides, Boc-(L-Leu-Aib)$_8$-OBzl takes more vertical orientation than the other longer peptides, Boc-(L-Leu-Aib)$_{12}$-OBzl

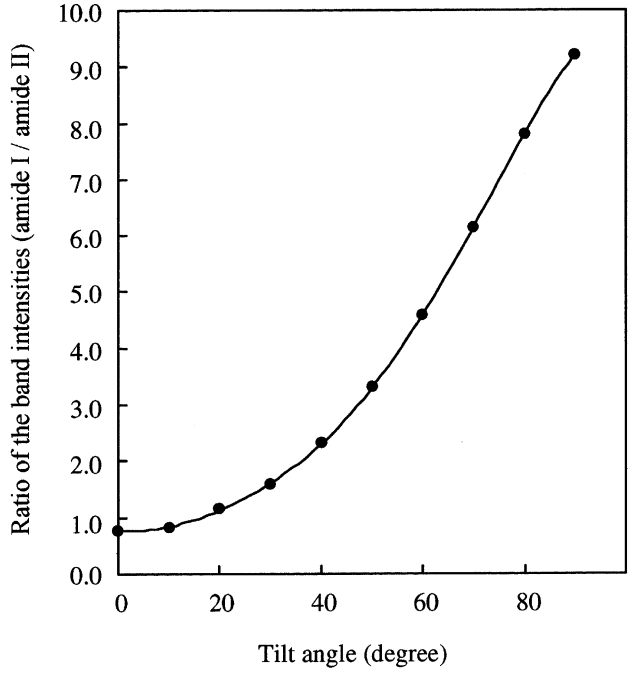

Fig. 4. The theoretically calculated relationship between tilt angles of helical peptides from surface normal and intensity ratios of amide I and II bands in RAS with using s-polarized light on water subphase.

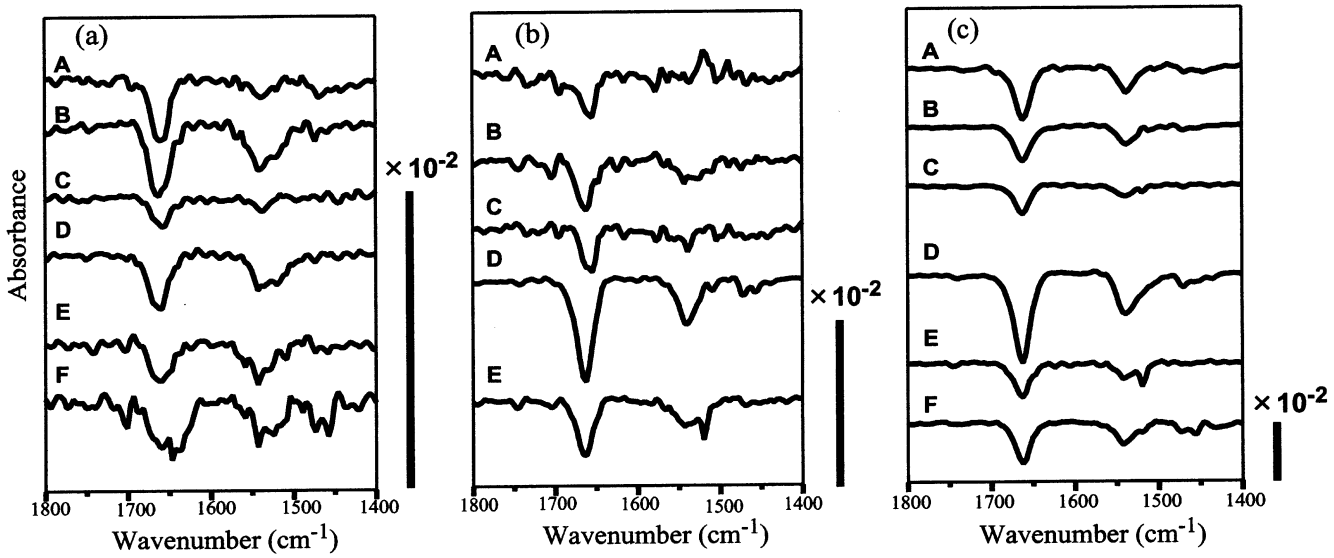

Fig. 5. FTIR-RAS spectra on subphase of (a) Boc-(L-Leu-Aib)$_8$-OBzl, (b) Boc-(L-Leu-Aib)$_{12}$-OBzl, and (c) Boc-(L-Leu-Aib)$_{16}$-OBzl monolayers prepared by various methods: (A) a chloroform solution of the peptide was spread on water at a molecular area of 1.5 nm^2; (B) a chloroform solution of the peptide was spread on water initially at a molecular area of 2.4 nm^2, and then compressed to that of 1.5 nm^2; (C) an *n*-butanol solution of the peptide was spread on water at a molecular area of 2.5 nm^2; (D) an *n*-butanol solution of the peptide was spread on water at a molecular area of 1.5 nm^2; (E) an *n*-butanol solution of the peptide was spread on water initially at a molecular area of 2.4 nm^2, and then compressed to a molecular area of 1.5 nm^2; (F) an *n*-butanol solution of the peptide was spread on a mixture of water and methanol at a molecular area of 1.5 nm^2.

and Boc-(L-Leu-Aib)$_{16}$-OBzl. The smallest tilt angle was observed for Boc-(L-Leu-Aib)$_8$-OBzl to be less than 30° when an *n*-butanol solution of Boc-(L-Leu-Aib)$_8$-OBzl was spread on water at a molecular area of 1.5 nm^2 or after a slight compression from 2.4 to 1.5 nm^2 of the Boc-(L-Leu-Aib)$_8$-OBzl monolayer prepared from a chloroform or an *n*-butanol solution. It is considered that the peptides at a gas phase take parallel orientation to the water surface due to the strong interaction with the surface, because each peptide has a free space to allow interaction with the surface, and the interaction should be too strong to induce change in the orientation by compression. However, when

Table 1
The intensity ratios of amide I and II bands and the tilt angles of the peptide monolayer prepared under various conditions

Peptide	Condition			Ratio of amide I/amide II	Tilt angle (deg)
	Spreading solution[a]	Molecular area (nm^2)	Subphase		
Boc-(L-Leu-Aib)$_8$-OBzl	*n*-Butanol	1.5	Water	1.47	28
		2.5	Water	2.35	40
		1.5[b]	Water	1.31	25
		1.5	Water/methanol[c]	1.25	23
	Chloroform	1.5	Water	3.16	48
		1.5[b]	Water	1.50	29
Boc-(L-Leu-Aib)$_{12}$-OBzl	*n*-Butanol	1.5	Water	2.30	39
		2.5	Water	2.57	42
		1.5[b]	Water	2.45	41
	Chloroform	1.5	Water	4.38	56
		1.5[b]	Water	2.24	39
Boc-(L-Leu-Aib)$_{16}$-OBzl	*n*-Butanol	1.5	Water	2.22	39
		2.5	Water	2.97	46
		1.5[b]	Water	2.03	36
		1.5	Water/methanol[c]	1.80	33
	Chloroform	1.5	Water	1.95	35
		1.5[b]	Water	2.43	41

[a] Concentration of each solution was 0.3 mM.
[b] Monolayer was compressed from a molecular area of 2.4–1.5 nm^2.
[c] Monolayer was spread on a mixture of water and methanol (1/1 v/v) subphase.

Table 2
The intensity ratios of amide I and II bands and the tilt angles (deg) of Boc-(L-Leu-Aib)$_8$-OBzl and Boc-(L-Leu-Aib)$_{16}$-OBzl layers formed on gold with changing the number of layers

Peptide	Water subphase[a]			Water/methanol subphase[b]		
	No. of layers	Amide I/amide II	Tilt angle (deg)	No. of layers	Amide I/amide II	Tilt angle (deg)
Boc-(L-Leu-Aib)$_8$-OBzl	1	0.77	78	1	2.36	45
	5	2.20	47	5	5.83	26
	10	2.27	46	10	8.93	17
Boc-(L-Leu-Aib)$_8$-OBzl	1	1.05	66	1	1.36	59
	4	1.19	63	5	1.62	54
	10	1.27	61	10	1.83	51

[a] The peptide layers were prepared from water subphase.
[b] The peptide layers were prepared from a mixture of water and methanol (1/1 v/v) subphase.

the peptides are spread at a liquid phase, they are crowded to hinder the free interaction with the surface, and the interaction of the hydrophilic peptide terminals with water subphase may exceed over the other interaction resulting in promotion of the vertical orientation. Using *n*-butanol as a spreading solvent, thus, should be helpful for vertical orientation, because *n*-butanol evaporates slowly on water subphase and intermolecular interaction of peptides is strengthened in this solvent.

The subphase was changed from water to a mixture of

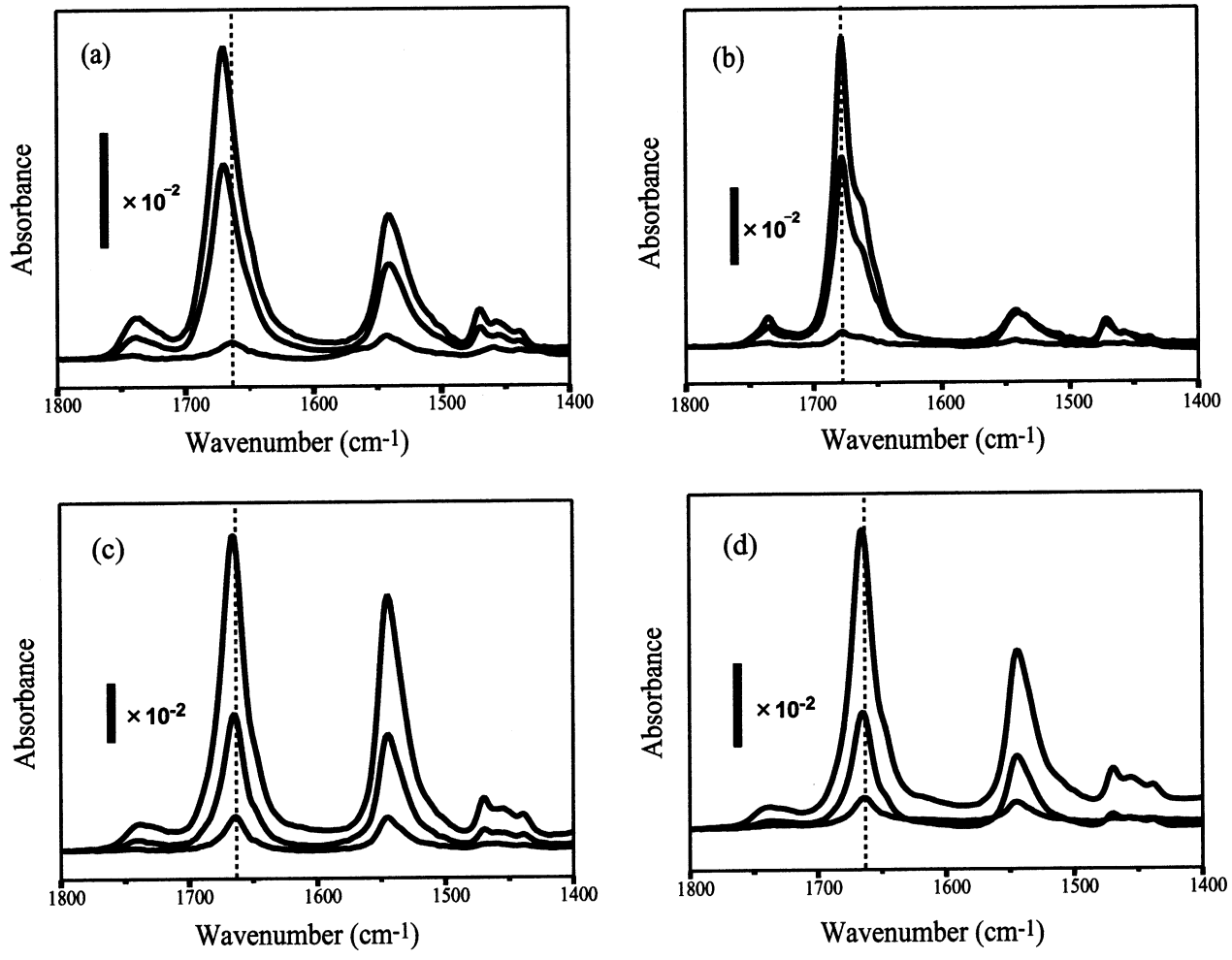

Fig. 6. FTIR-RAS spectra of the peptide multilayers deposited on gold. Each figure contains three spectra of monolayer, five-layer (four-layer in (c)), and 10-layer in the order of the peak intensity. (a) and (b) show RAS spectra of Boc-(L-Leu-Aib)$_8$-OBzl layers on gold transferred from the peptide monolayer spread on water and on a mixture of water and methanol, respectively. (c) and (d) show RAS spectra of Boc-(L-Leu-Aib)$_{16}$-OBzl layers on gold transferred from the peptide monolayer spread on water and on a mixture of water and methanol, respectively.

water and methanol (1/1 v/v), and the effect of subphase on the monolayer formation of helical peptides was investigated. Methanol was used for its low dielectric constant and no absorption in the range from 1500 to 1700 cm^{-1} of IR measurements. The latter property allows the application of the relationship (Fig. 4) to peptide monolayers even on the water/methanol subphase.

An *n*-butanol solution of Boc-(L-Leu-Aib)$_8$-OBzl or Boc-(L-Leu-Aib)$_{16}$-OBzl was spread on a mixture of water and methanol at a molecular area of 1.5 nm^2. As shown in Table 1, the tilt angles of the peptide monolayers become smaller than those of using water as subphase. Especially in the case of Boc-(L-Leu-Aib)$_8$-OBzl monolayer, the tilt angle was as low as 23°. One of the reasons for the preferential vertical orientation on a mixture of water and methanol should be its low dielelctric constant, where the electrostatic interaction of the helical peptide with the image dipole in the subphase is significantly reduced. Parallel orientation of the helices to the surface brings the closest contact of the peptide with the image dipole that maximizes the electrostatic interaction. The tendency of the parallel orientation should, therefore, be weakened with lowering the dielectric constant of the subphase. Another reason might be lower surface tension by mixing methanol to water, which promotes association of the peptides on the surface resulting in decrease of the relative contribution of the peptide–surface interaction to the orientation of the helices at the interface.

3.4. Peptide layers on gold

The peptide monolayers were transferred on gold and investigated by RAS measurement. When the peptide monolayers on subphase were transferred on gold by the horizontal dipping method, in most cases the orientation of the peptides were closely to horizontal to the gold surface even though the peptides took vertical orientation on subphase. However, vertically oriented peptide layers on gold were obtained by a different method, where the subphase was put directly on gold, and the peptide monolayer formed on the subphase was transferred on gold by evaporation of the subphase at 40 °C. On repeating this procedure, multilayers of helical peptides were obtained as shown by increase of the amide I band intensity by RAS measurement (Fig. 6). The tilt angles of helices on gold were calculated from the intensity ratios of amides I and II bands according to the method reported previously [9] and are summarized in Table 2. Interestingly, average tilt angles of the multilayers become smaller as the layer number increases. This tendency was observed with either Boc-(L-Leu-Aib)$_8$-OBzl or Boc-(L-Leu-Aib)$_{16}$-OBzl using either water or water/methanol as subphase. The smallest tilt angle of 17° was obtained with 10 layers of Boc-(L-Leu-Aib)$_8$-OBzl prepared by using water/methanol as subphase. This combination, Boc-(L-Leu-Aib)$_8$-OBzl using water/methanol as subphase, coincides with that giving the smallest tilt angle on subphase, suggesting that vertical orientation on subphase should be preserved after removal of the subphase under the condition. The peak shift of amide I band to higher wavenumber 1678 cm^{-1} was observed with the 10 layers of Boc-(L-Leu-Aib)$_8$-OBzl, which also supports the vertical orientation of the peptide. The large shift is due to the LO–TO coupling of the vertically oriented membrane [25].

The smaller tilt angle with thicker peptide layer may be explained similarly to the above speculation that the electrostatic interaction of the peptide with the mirror image is diminished with increasing the distance separating the monolayer and gold. The vertical orientation of peptides should be obtained under less interaction with surface and stronger intermolecular interaction among peptides.

4. Conclusion

Molecular assembling is one of the key methods for the nanotechnology. Formation of a unique structure by assembling organic molecules is indispensable for a specific function of nanodevices. Organic molecules, which are designed for such purposes, are usually equipped with functional groups such as charged species and dipolar chromophores. Those groups must be organized regularly for example on gold substrate. In these cases, the strong electrostatic interaction with the image charge or dipole will significantly influence the molecular organization as shown here. Helical peptides are interesting for the large dipole moment and are shown here successfully organized in a vertical orientation on liquid or gold surface. These molecular assemblies composed of vertically oriented helical peptides will show good properties suitable for nanomaterials showing pyroelectricity, piezoelectricity, and second harmonic generation, etc.

Acknowledgements

This work was partially supported by Grand-in-Aid for Scientific Research B (12450372) and Priority Areas Research B (Construction of Dynamic Redox Systems Based on Nano-Space Control).

References

[1] Fujita K, Kimura S, Imanishi Y, Rump E, Ringsdorf H. Langmuir 1994;10:2731–5.
[2] Fujita K, Kimura S, Imanishi Y, Rump E, Ringsdorf H. Langmuir 1995;11:253–8.
[3] Kimura S. Molecular organization of peptides and their function. In: Nalwa HS, editor. Handbook of surfaces and interfaces of materials, vol. 5. San Diego: Academic Press, 2001. p. 207–31.
[4] Fujita K, Kimura S, Imanishi Y, Okamura E, Umemura J. Langmuir 1995;11:1675–9.
[5] Worley CG, Linton RW, Samulski ET. Langmuir 1995;11:3805–10.
[6] Boncheva M, Vogel H. Biophys J 1997;73:1056–72.

[7] Miura Y, Kimura S, Imanishi Y, Umemura J. Langmuir 1998;14:6935–40.
[8] Miura Y, Kimura S, Imanishi Y, Umemura J. Langmuir 1998; 14:2761–7.
[9] Miura Y, Kimura S, Imanishi Y, Umemura J. Langmuir 1999; 15:1155–60.
[10] Miura Y, Xu G-C, Kimura S, Kobayashi S, Iwamoto M, Imanishi Y, Umemura J. Thin Solid Films 2001;393:59–65.
[11] Kinoshita K, Doi T, Mori T, Okahata Y. Chem Lett 1998:951–2.
[12] Schwyzer R. Biopolymers 1995;37:5–16.
[13] Doi T, Kinoshita T, Tsujita Y, Yoshimizu H. Bull Chem Soc Jpn 2001;74:421–5.
[14] Sugimura A, Iwamoto M, Zhong-can O-Y. Phys Rev E 1994;50:614–7.
[15] Otoda K, Kitagawa Y, Kimura S, Imanishi Y. Biopolymers 1993; 33:1337–45.
[16] Sakai H, Umemura J. Langmuir 1998;14:6249–55.
[17] Ohta K, Ishida H. Appl Opt 1990;29:1952–9.
[18] Abeles F. Ann Phys 1948;3:504–20.
[19] Hansen WN. J Opt Soc Am 1968;58:380–90.
[20] Bertie JE, Ahmed MK. J Phys Chem 1989;93:2210–8.
[21] Miyazawa T. J Chem Phys 1961;35:693–713.
[22] Buffeteau T, Le Calvez E, Castano S, Desbat B, Blaudez D, Dufourcq J. J Phys Chem B 2000;104:4537–44.
[23] Buffeteau T, Le Calvez E, Desbat B, Pelletier I, Pezolet M. J Phys Chem B 2001;105:1464–71.
[24] Ohta K, Ishida H. Appl Spectrosc 1988;42:952–7.
[25] Miura Y, Kimura S, Kobayashi S, Iwamoto M, Imanishi Y, Umemura J. Chem Phys Lett 1999;315:1–6.